

Application of Z_{eff} Profile Analysis Based on Visible Bremsstrahlung Measurement to Different Density Profiles in the LHD

Hangyu ZHOU, Shigeru MORITA¹⁾, Motoshi GOTO¹⁾, Kazumichi NARIHARA¹⁾
and Ichihiko YAMADA¹⁾

Department of Fusion Science, Graduate University for Advanced Studies, Toki 509-5292, Gifu, Japan

¹⁾*National Institute for Fusion Science, Toki 509-5292, Gifu, Japan*

(Received 11 January 2009 / Accepted 8 June 2009)

Visible bremsstrahlung emission has been measured along the vertical direction of a horizontally elongated plasma cross section in a range of $-0.6\text{ m} \leq z \leq 0.0\text{ m}$ from an inwardly shifted ($R_{\text{ax}} \leq 3.6\text{ m}$) configuration by means of an optimized Czerny-Turner spectrometer installed on the Large Helical Device. Chord-integrated bremsstrahlung intensity profiles have been observed in discharges having no asymmetric strong edge bremsstrahlung emission originating in the ergodic layer. Radial bremsstrahlung emission profiles are obtained from the chord-integrated profiles based on an Abel inversion method. Z_{eff} profiles are thus analyzed for peaked, flat, and hollow density profiles, which are measured with a Thomson scattering diagnostic, as the first trial of the analysis. As a result, a flat Z_{eff} profile is obtained for all different density profiles with values of $1 < Z_{\text{eff}} \leq 2$. This indicates that the partial impurity pressure is essentially constant against the plasma radius.

© 2010 The Japan Society of Plasma Science and Nuclear Fusion Research

Keywords: Z_{eff} profile, visible bremsstrahlung, density profile

DOI: 10.1585/pfr.5.S1021

1. Introduction

Plasma fuel dilution and enhanced radiation loss caused by impurity buildup are still serious problems in fusion research with magnetic confinement. Therefore, the study of impurity transport becomes important for understanding the behavior of impurities and improving plasma performance [1, 2]. In the Large Helical Device (LHD), a variety of electron density profiles, such as peaked, flat, and hollow profiles, have been observed under different experimental conditions; they are quite different from the density profile usually seen in tokamaks, i.e., a peaked profile. It is very interesting to study the impurity transport at such different density profiles in the LHD and to compare it with the tokamak case. For this purpose, the use of Z_{eff} profiles has been considered in the LHD to obtain necessary information on impurity transport, especially in the plasma core region.

Visible bremsstrahlung emission has been measured along the vertical direction of a horizontally elongated plasma cross section with an optimized Czerny-Turner visible spectrometer [3] installed on the LHD. The full vertical chord-integrated visible bremsstrahlung profile is observable, including the upper and lower edge emission, in a range of $-0.6\text{ m} \leq z \leq 0.6\text{ m}$. The instrument can entirely eliminate line emission from the bremsstrahlung signal, which was a serious problem in old bremsstrahlung measurement systems with an interference filter [4]. The new visible spectrometer system consists of a 44-fiber ar-

ray, an astigmatism-corrected Czerny-Turner visible spectrometer, and a charge-coupled device (CCD). The vertical spatial and time resolutions are 30 mm and 100 ms, respectively. However, an asymmetric bremsstrahlung profile has still been observed after changing the diagnostic system. Detailed data analysis revealed that the asymmetric part of the signal originates in strong edge bremsstrahlung emission from a thick ergodic layer, since all the observation chords include the edge emission. Fortunately, we could confirm that the lower half of the full vertical bremsstrahlung profile was not influenced by the edge emission in inwardly shifted magnetic configurations ($R_{\text{ax}} \leq 3.6\text{ m}$), where the ergodic layer is relatively thin. The local bremsstrahlung emission profile is obtained from chord-integrated signals through an Abel inversion, assuming an elliptical magnetic surface with the finite- β effect. The Z_{eff} profile is finally obtained, taking into consideration electron density and temperature profiles measured by a Thomson scattering diagnostic [5]. In this paper, the Z_{eff} profiles from the LHD are presented for three different density profiles as the first trial of the data analysis.

2. Experimental Setup

The Czerny-Turner visible spectrometer consists of a toroidal mirror, a flat mirror, two spherical mirrors, and three gratings, as shown in Fig. 1. A short focal length of 300 mm is adopted to achieve an extremely bright system. The three gratings, with 120 (blaze: 330 nm), 300 (500 nm), and 1200 (200 nm) grooves/mm, are set in the

author's e-mail: Zhou.hangyu@nifs.ac.jp

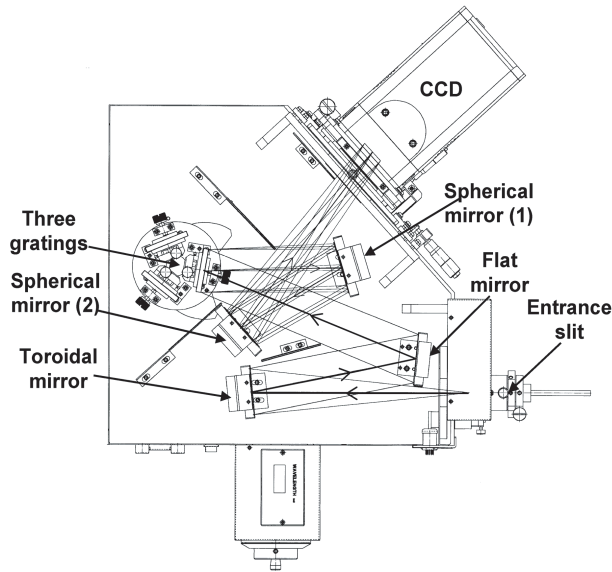


Fig. 1 Optical arrangement of 300-mm Czerny-Turner visible spectrometer. Light path is indicated by black arrow.

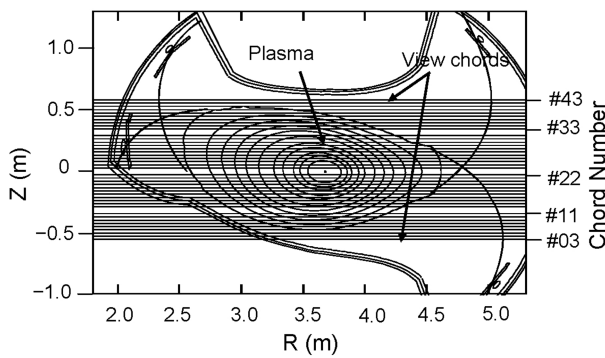


Fig. 2 Fiber array arrangement in the LHD (R : major radius of torus, Z : vertical distance from equator plane). Fiber array consists of 44 fibers, and fiber chords from #3 to #43 are traced.

turret. In typical LHD experiments, the 300 grooves/mm grating is used mainly to observe a wider wavelength range of 500 nm to 600 nm with higher spectral resolution. Figure 2 shows parallel view chords at a horizontally elongated plasma cross section. Emission from the plasma is observed by the vertical fiber array, which measures the height in the range $-0.6 \text{ m} \leq z \leq 0.6 \text{ m}$. The fiber array consists of 44 quartz optical fibers with a core diameter of 100 μm and clad diameter of 125 μm . The spatial resolution of 30 mm at the plasma center is defined by an optical lens with a focal length of 30 mm, which is coupled with each optical fiber. Output spectra are detected by a CCD. The CCD has a detection area of $13.3 \times 13.3 \text{ mm}^2$ (1024×1024 pixels, $13 \times 13 \mu\text{m}^2/\text{pixel}$). It is usually operated at -20°C to reduce thermal noise. An exposure time of 31 ms and temporal resolution of 100 ms are selected in the present study, with a readout speed of 11 $\mu\text{s}/\text{line}$ and 0.4 $\mu\text{s}/\text{pixel}$. The exposure time is exactly defined by a mechanical shutter placed in front of the CCD.

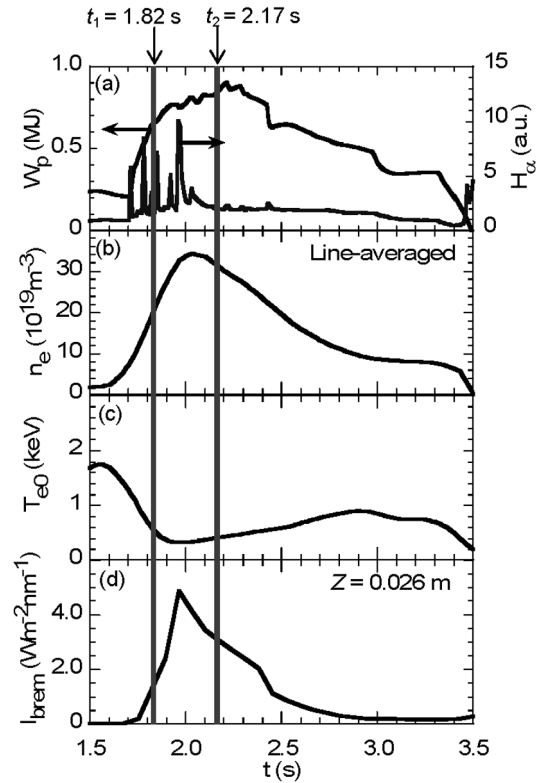


Fig. 3 Waveforms of high-density discharge with multi-pellet injection for peaked density profile: (a) Plasma stored energy W_p and H_α intensity, (b) Line-averaged electron density \bar{n}_e , (c) Central electron temperature T_{e0} , and (d) Chord-integrated bremsstrahlung emission I_{brem} . Z_{eff} profiles are analyzed at two different time slices, $t_1 = 1.82 \text{ s}$ and $t_2 = 2.17 \text{ s}$, indicated by vertical lines.

3. Analysis of Radial Z_{eff} Profile

Density profiles in the LHD change according to the heating power, magnetic field strength, magnetic axis position, and fueling method. A peaked density profile is easily produced by hydrogen multi-pellet injection. The Z_{eff} profile is analyzed for a peaked density profile formed in the high-density range with pellet injection. Figure 3 shows typical waveforms: (a) plasma stored energy W_p and H_α intensity, (b) line-averaged electron density \bar{n}_e , (c) central electron temperature T_{e0} , and (d) chord-integrated bremsstrahlung emission I_{brem} .

Ten H_2 pellets were successively injected along magnetic axis of 3.85 m from 1.70–2.02 s. Plasma energy quickly increased during pellet injection and reached 0.9 MJ. The line-averaged electron density, evaluated from the density profile measured with Thomson scattering, continuously increased and reached $3.5 \times 10^{20} \text{ m}^{-3}$, whereas the electron temperature in the plasma center decreased drastically to 0.3 keV. Chord-integrated bremsstrahlung emission also increased in the same manner and reached quite a large value of $4.9 \text{ Wm}^{-2} \text{ nm}^{-1}$. Here, the β value increased greatly, becoming 1.13 %.

At 1.82 s after the third pellet injection, the radial Z_{eff}

profile was analyzed with electron density and temperature profiles in addition to the local bremsstrahlung emissivity calculation based on the Abel inversion technique with $\beta = 1.07\%$. Figure 4 shows the radial distribution of plasma parameters for a super-dense core (SDC) plasma at $t_1 = 1.82$ s: (a) electron density n_e , (b) electron temperature T_e , (c) Abel-inverted bremsstrahlung emissivity $\varepsilon_{\text{brem}}$, and (d) Z_{eff} from the above measurement. The radial distribution of $Z_{\text{eff}}(\rho)$ in Fig. 4(d) is calculated based on the above three values: $n_e(\rho)$, $T_e(\rho)$, and $\varepsilon_{\text{brem}}(\rho)$. The temperature profile is entirely flat at $\rho < 0.8$ and quickly decreases at $\rho > 0.8$. The outside boundary of the edge temperature expands to $\rho = 1.2$ in the ergodic layer. The bremsstrahlung emissivity profile is also peaked, like the density profile. The Z_{eff} profile analyzed from the peaked density profile is fairly flat in the core plasma region inside $\rho = 1.0$. The analysis of the Z_{eff} profile can be extended to $\rho \sim 1.13$. However, it is difficult to analyze Z_{eff} exactly, because uncertainties in the density and temperature profiles of Thomson scattering become large in the

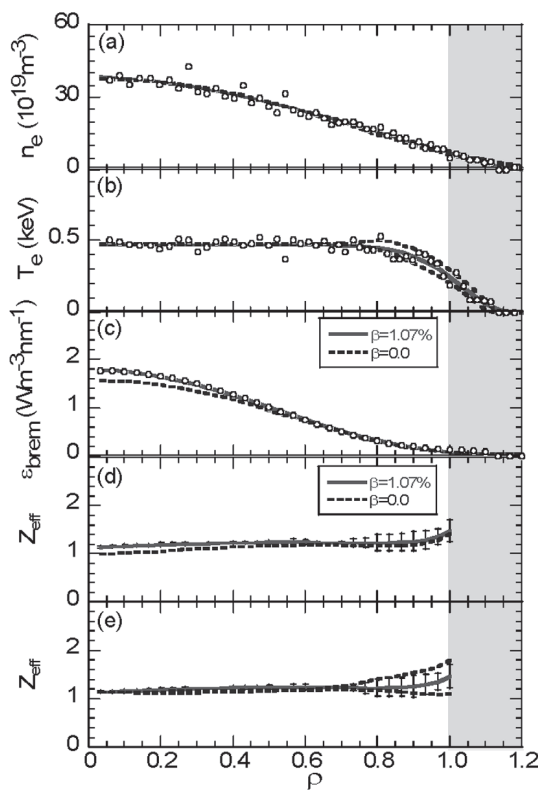


Fig. 4 Radial profiles of plasma parameters for a peaked density distribution as a function of normalized radius ρ at $t_1 = 1.82$ s, indicated in Fig. 3, during multi-pellet injection: (a) Electron density n_e , (b) Electron temperature T_e , (c) Bremsstrahlung emissivity after Abel inversion $\varepsilon_{\text{brem}}$, (d) Calculated effective ion charge from the above measurement of Z_{eff} for different magnetic surfaces, and (e) Calculated effective ion charge Z_{eff} with uncertainty due to scattered Thomson data. Dashed lines in (a), (b), and (e) indicate the uncertainty of the corresponding profile.

ergodic layer, which is denoted with square hatch marks in Fig. 4. The error bars of the Z_{eff} profile originating in the density and temperature profiles are quite small inside $\rho = 0.7$ but gradually increase at the edge plasmas, e.g., 23% at $\rho = 1.0$. The fitting curves for electron density and temperature profiles used in the present analysis are also indicated in Figs. 4 (a) and (b). Another important point regarding the uncertainty of the Z_{eff} profile is in the selection of a magnetic surface deformed by plasma pressure. The magnetic surface is of course necessary for Abel inversion of the line-integrated bremsstrahlung signal.

Figure 5 shows (a) n_e , (b) T_e , (c) $\varepsilon_{\text{brem}}$, and (d) Z_{eff} at 2.17 s, just after pellet injection ends, indicated by a vertical line in Fig. 3. The radial bremsstrahlung emissivity is calculated based on the Abel inversion technique with $\beta = 1.94\%$. The electron density profile is more peaked with a higher density at the plasma core, and the outside density boundary is close to $\rho = 1.0$. This means the plasma size has shrunk. Meanwhile, the electron temperature is slightly lower than that at 1.82 s, but the profile is still flat. The bremsstrahlung emissivity profile then becomes more peaked than the density profile, as seen in

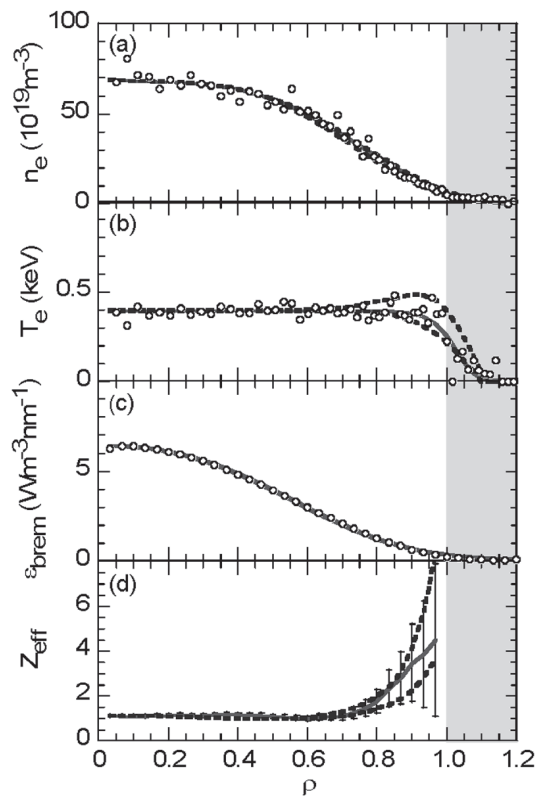


Fig. 5 Radial profiles of plasma parameters for a peaked density distribution as a function of normalized radius ρ at $t_2 = 2.17$ s, indicated by a vertical line in Fig. 3, after multi-pellet injection and super-dense core (SDC) plasma formation (a) n_e , (b) T_e , (c) $\varepsilon_{\text{brem}}$, and (d) Z_{eff} with uncertainty due to scattered Thomson data. Dashed lines in (a), (b), and (d) indicate the uncertainty of the corresponding profile.

Fig. 5 (c). The analyzed Z_{eff} profile shown in Fig. 5 (d) seems to also be flat, at least inside $\rho = 0.7$, and the values are distributed around 1.11. Although the error bars of Z_{eff} are quite small inside $\rho = 0.7$, they quickly increase with plasma radius. The error bars of Z_{eff} , caused only by uncertainty of the Thomson data, indicated by two dashed lines in Figs. 5 (a) and (b), are shown with dashed lines in Fig. 5 (d). However, these error bars of Z_{eff} , due to the edge density and temperature profiles, are about 50 % of the total enlarged error bars outside of the plasma. The other source of error is quite unclear at present. As a possible source, we consider that these enlarged error bars originate in the magnetic surface structure used in the analysis. In SDC plasmas, an extremely large magnetic axis shift has been observed after pellet injection. It is then difficult to solve the magnetic surface structure in the usual way using VMEC calculation [6]. Further theoretical study of magnetohydrodynamic (MHD) equilibrium is now being carried out to find accurate magnetic surface structure in such SDC plasmas with extremely peaked pressure profiles.

The uncertainty of the Z_{eff} profile due to magnetic surface deformation is checked at the plasma core using two different magnetic surfaces with $\beta = 0$ and 1.07 %. The plasma axis shift used in the analysis is 0.2 m when $\beta = 1.07$ %. Two bremsstrahlung emissivity profiles obtained from the two magnetic surfaces, shown in Fig. 4 (c), are quite similar, whereas a small difference appears in the plasma core. Since the visible bremsstrahlung emission is horizontally observed from the outboard side of the torus, the effect on the magnetic surface distortion becomes much less than that in vertical measurement. In particular, the difference in the Z_{eff} value can be neglected in the outer plasma region, because magnetic surface distortion occurs mainly in the plasma core. This strongly suggests that the uncertainty in the Z_{eff} profile on the assumed magnetic surface is quite small, at least in the plasma core, compared to that of the density and temperature profiles in the present diagnostic system with the exception of SDC plasmas. Another uncertainty of the Z_{eff} profile at the edge ($\rho \geq 0.75$) due to scattered Thomson data is shown with dashed lines in Fig. 4 (e). The uncertainty of the density and temperature profiles are shown with dashed lines in Figs. 4 (a) and (b), respectively. It is finally found that errors in the Z_{eff} profile are caused mainly by scattered Thomson data for the plasma at 1.82 s. In particular, the uncertainty of the edge density profile has a large effect on Z_{eff} error estimation, whereas the edge profile data are not scattered, as seen in Fig. 4 (a).

Next, the Z_{eff} profile is analyzed for a flat density profile. The data are taken from stable plasma discharge at $R_{\text{ax}} = 3.6$ m. Figure 6 shows the discharge waveforms of SN#85124: (a) plasma stored energy W_p , (b) line-averaged electron density \bar{n}_e , (c) central electron temperature T_{e0} , and (d) chord-integrated bremsstrahlung emission I_{brem} at $Z = 0.026$ m. The plasma energy is constantly sustained from 0.8 s to 3.3 s. The line-averaged electron density is

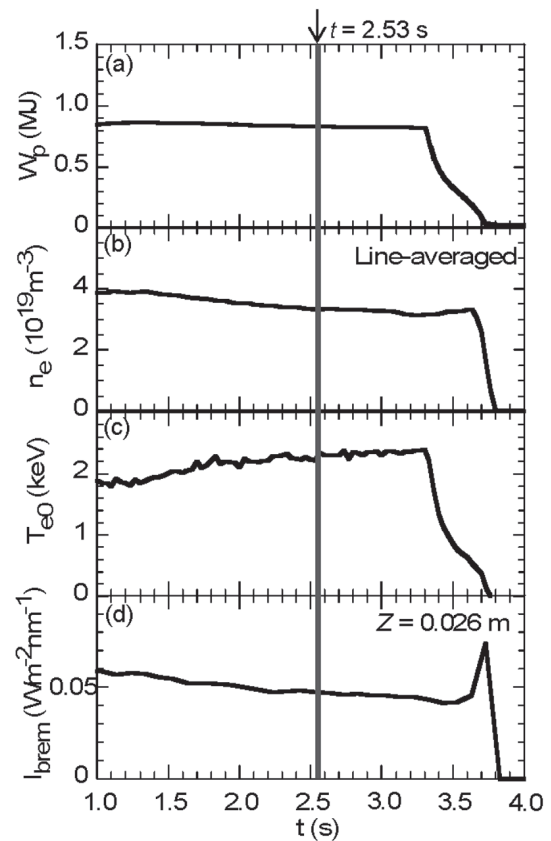


Fig. 6 Waveforms of stable discharge for flat density profile: (a) W_p , (b) \bar{n}_e , (c) T_{e0} , and (d) I_{brem} .

kept at roughly $3.5 \times 10^{19} \text{ m}^{-3}$, and the central electron temperature increases slightly, from 2.0 keV to 2.2 keV, during the steady phase according to the gradual decrease in the density. The chord-integrated bremsstrahlung emission behaves similarly to the density. The β value is 0.88 % at the steady phase. Figure 7 shows radial profiles of (a) n_e , (b) T_e , (c) $\varepsilon_{\text{brem}}$, and (d) Z_{eff} at 2.53 s in Fig. 6. The density profile is entirely flat at $\rho < 0.9$, whereas the temperature profile is peaked. The bremsstrahlung emissivity profile after Abel inversion becomes slightly hollow. This indicates that there is little temperature dependence in the visible bremsstrahlung emission. The Z_{eff} profile is flat, with values near 2.05. Analysis in the ergodic layer is still difficult. The error bars of the Z_{eff} profile gradually increase toward the plasma core; the maximum error bar appears as 12 % at the plasma center. Clearly, the increase in the error bars at the plasma core originates in the local emissivity calculation of the bremsstrahlung based on the Abel inversion method, in addition to error bars from density profile fitting from $0.2 < \rho < 0.4$.

The hollow density profile is observed in the density rise phase at $R_{\text{ax}} = 3.60$ m. Figure 8 shows the discharge waveforms. The line-averaged electron density gradually increases from 0.5 to 1.5 s and finally reaches $6 \times 10^{19} \text{ m}^{-3}$, although the plasma energy remains constant. The central plasma temperature then decreases from

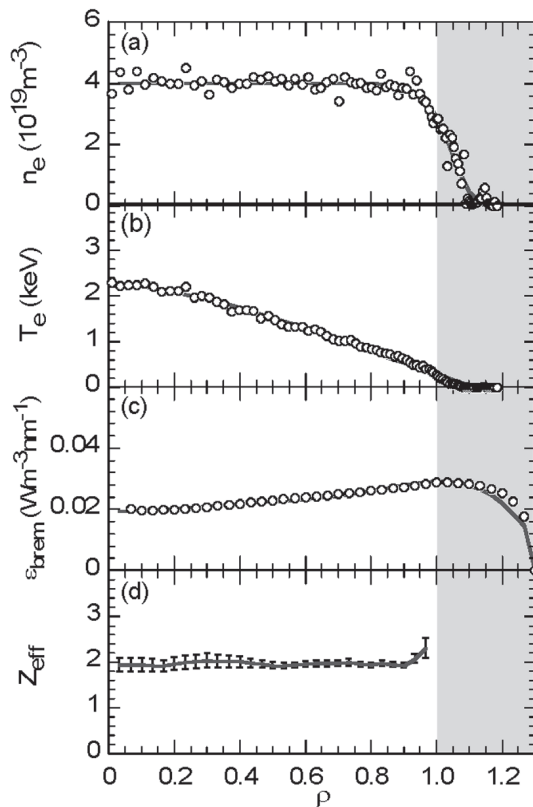


Fig. 7 Radial profiles as a function of normalized radius ρ at $t = 2.53$ s, indicated by a vertical line in Fig. 6: (a) n_e , (b) T_e , (c) ϵ_{brem} , and (d) Z_{eff} .

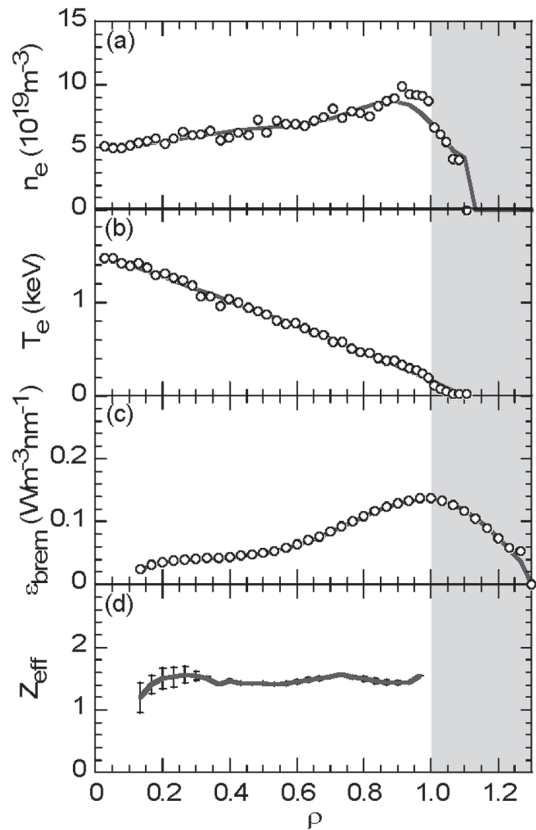


Fig. 9 Radial profiles at 1.13 s, indicated by a vertical line in Fig. 8, as a function of normalized radius ρ : (a) n_e , (b) T_e , (c) ϵ_{brem} , and (d) Z_{eff} .

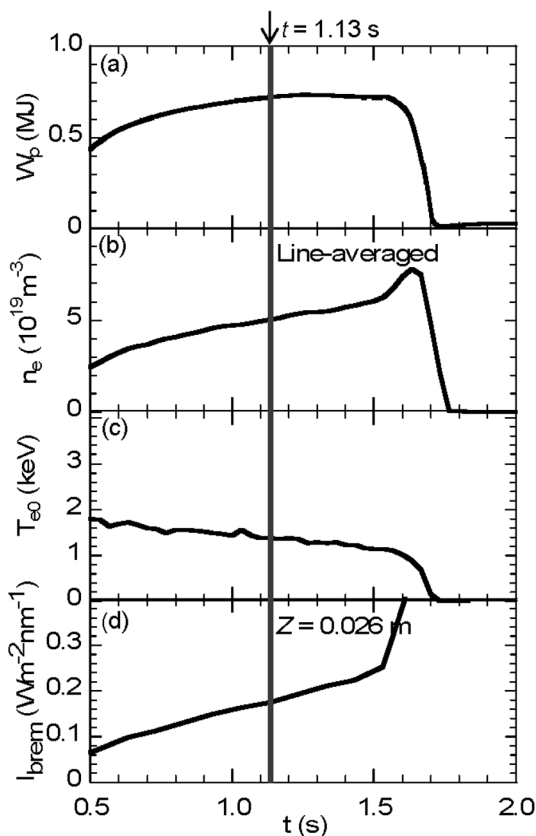


Fig. 8 Waveforms of density rise discharge for hollow density profile: (a) W_p , (b) \bar{n}_e , (c) T_{e0} , and (d) I_{brem} .

1.8 to 1.2 keV. The chord-integrated bremsstrahlung emission also increases according to the density rise. The β value is 0.58 % in the discharge. Figure 9 depicts radial profiles of (a) n_e , (b) T_e , (c) ϵ_{brem} , and (d) Z_{eff} at 1.13 s in Fig. 8. A hollow density profile forms, having its peak value at $\rho = 0.9$. In contrast, the temperature profile is peaked and forms a triangular shape. The bremsstrahlung emissivity decreases greatly at the plasma core, and the profile becomes hollower than the density profile. The Z_{eff} profile is also flat, with values around 1.58. In the case of a hollow density profile, analysis is generally difficult because of relatively large error bars in the density profile and difficulty in calculating the Abel inversion. The error bars in the Z_{eff} profile also increase in this case, i.e., $\sim 30\%$, at the plasma core. At present, therefore, the detailed structure in the Z_{eff} profile cannot be discussed.

4. Summary and Discussion

Z_{eff} profiles from visible bremsstrahlung measurement are analyzed for peaked, flat, and hollow density profiles in LHD plasmas. An essentially flat Z_{eff} profile is obtained for all different density profiles. This indicates that the impurity partial pressure is constant in typical LHD discharges. The error bars seen in the Z_{eff} profiles originate mainly in fitting curves to express the electron temperature and den-

sity profiles and in calculating the Abel inversion calculation. The uncertainty in magnetic surface distortion is relatively small except for SDC plasmas. More precise Z_{eff} profile analysis will be done after optimizing the magnetic surface used in the calculation and modifying the method of calculating the Abel inversion.

Acknowledgments

The authors thank the members of the LHD experimental group for LHD operation. This work was carried out in part with the LHD project's financial support (NIFS08ULPP527). This work was also partly supported

by the JSPS-CAS Core University Program in the field of "Plasma and Nuclear Fusion".

- [1] D. P. Schissel *et al.*, Phys. Fluids **31**, 3738 (1988).
- [2] S. Morita, M. Goto *et al.*, Physica Scripta **T91**, 48 (2001).
- [3] H. Y. Zhou, S. Morita, M. Goto and M. B. Chowdhuri, Rev. Sci. Instrum. **79**, 10F536 (2008).
- [4] H. Nozato, S. Morita and M. Goto, J. Plasma Fusion Res. **5**, 442 (2002).
- [5] K. Narihara *et al.*, Rev. Sci. Instrum. **72**, 1122 (2001).
- [6] S. P. Hirshman, W. I. van Rij and P. Merkel, Comput. Phys. Commun. **43**, 143 (1986).